JACS
JOURNAL OF THE AMERICAN CHEMICAL SOCIETY

Article

pubs.acs.org/JACS

A Working Hypothesis for Broadening Framework Types of Zeolites in Seed-Assisted Synthesis without Organic Structure-Directing Agent

Keiji Itabashi, Yoshihiro Kamimura, Kenta Iyoki, Atsushi Shimojima, and Tatsuya Okubo*

Department of Chemical System Engineering, The University of Tokyo, 7-3-1 Hongo, Bunkyo-ku, Tokyo 113-8656, Japan

Supporting Information

ABSTRACT: Recent research has demonstrated a new synthesis route to useful zeolites such as beta, RUB-13, and ZSM-12 via seed-assisted, organic structure-directing agent (OSDA)-free synthesis, although it had been believed that these zeolites could be essentially synthesized with OSDAs. These zeolites are obtained by adding seeds to the gels that otherwise yield other zeolites; however, the underlying crystallization mechanism has not been fully understood yet. Without any strategy, it is unavoidable to employ a trial-and-error procedure for broadening zeolite types by using this synthesis method. In this study, the effect of zeolite seeds with different framework structures is investigated to understand the crystallization mechanism of zeolites obtained by the seed-assisted, OSDA-free synthesis method. It has been found that the key factor in the successful synthesis of zeolites in the absence of OSDA is the common composite building unit contained both in the seeds and in the zeolite obtained from the gel after heating without seeds. A new working hypothesis for broadening zeolite types by the seed-assisted synthesis without OSDA is proposed on the basis of the findings of the common composite building units in zeolites. This hypothesis enables us to design the synthesis condition of target zeolites. The validity of the hypothesis is experimentally tested and verified by synthesizing several zeolites including ECR-18 in K−aluminosilicate system.

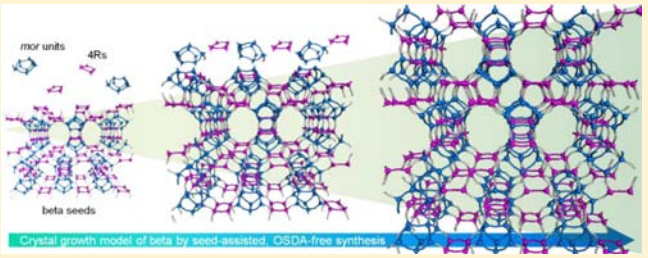

INTRODUCTION

Aluminosilicate zeolites are crystalline microporous materials with three-dimensional framework structures consisting of tetrahedrally coordinated $SiO_{4/2}$ and $AlO_{4/2}$ units, which have been widely used as adsorbents, catalysts, and ion-exchangers. Their high microporosity as well as solid acidity, adsorption−desorption properties of organic and inorganic molecules, and ion-exchange properties ascribed to the well-defined channel systems of these materials have been effectively utilized in diverse applications.[1−4] In the early days of zeolite synthesis, A, X, Y, L, mordenite, and so on were hydrothermally synthesized from aluminosilicate gels without using any organic structure-directing agent (OSDA), and these zeolites have been practically used worldwide. On the other hand, aluminosilicate zeolites with higher SiO_2/Al_2O_3 ratios have not been obtained from gels containing metal cations only. By employing bulky OSDAs, such as tetraalkylammonium ions, various aluminosilicate zeolites with higher SiO_2/Al_2O_3 ratios, such as ZSM-5, ZSM-11, ZSM-12, Theta-1, and beta, were found, which had the novel framework structures when first synthesized. Some of these new materials opened numerous, new catalytic applications in oil refining and the petrochemical industry, which means that the new zeolitic materials have high potential in catalysis and adsorption. New challenges in the synthesis of novel zeolites are presently continued by using OSDAs; however, these OSDAs are structurally complex and costly. From a practical viewpoint, the amount of OSDA should be reduced as much as possible because of the high cost, the complex synthesis processes, the consumption of energy for the removal of OSDA in the zeolite by calcination, and the high environmental burden of waste treatment. Therefore, an improved methodology for OSDA-free or simple synthesis with conventional OSDAs is strongly desired.

Recently, the seed-assisted, OSDA-free synthesis of important zeolites such as beta,[5−7] nanosized ZSM-5,[8] RUB-13,[9] ZSM-12,[10,11] and high-silica ferrierite[12] has been reported by several research groups. Xiao and co-workers proposed the core−shell growth mechanism for the seed-assisted synthesis of beta.[13] On the other hand, in our previous paper on the crystallization behavior of beta,[14] it was found that the beta seeds in the Na−aluminosilicate gel system were partially dissolved during hydrothermal treatment, and new beta crystallized on the surface of the residual beta seeds after the seeds were exposed to liquid and/or dispersed at the interface of the amorphous aluminosilicate and liquid. In this synthesis system, beta crystallized only when beta seeds were added, while mordenite was crystallized from the seed-free gel after prolonged hydrothermal treatment.[7] The seed-assisted synthesis of various zeolites has been widely studied to shorten the crystallization time or to improve the quality of the product zeolite since the early days;[15−19] however, the exact role of the

Received: March 6, 2012
Published: June 21, 2012

   dx.doi.org/10.1021/ja3022335 | J. Am. Chem. Soc. 2012, 134, 11542−11549

seeds and the crystallization mechanism have not been fully understood yet as well as in the case of the recent OSDA-free synthesis of beta.

To understand the detailed crystallization behavior of zeolites in the seed-assisted, OSDA-free synthesis, it is necessary to clarify the exact role of the seeds in combination with the reactant gel to which the seeds are added. In the present study, the effect of seeds with different zeolitic framework structures is comprehensively examined by focusing on the combination with a Na−aluminosilicate gel having the same chemical composition as that used in the OSDA-free synthesis of beta. When mordenite seeds are added, mordenite crystallizes at a strikingly rapid rate, and ferrierite is rapidly obtained by the addition of ferrierite seeds. On the basis of these results, a structural investigation was carried out to find the key factors that accelerate the crystallization rate of these zeolites by seeding. We assumed that the key factor is the composite building unit commonly contained in the frameworks of zeolite seeds and the crystallizing zeolite obtained from the seed-free gel. Here, we report and discuss in detail the results of the seed-assisted, OSDA-free synthesis of zeolites and a new working hypothesis, and present examples of broadening zeolite types by using the new hypothesis.

EXPERIMENTAL SECTION

Materials. The following raw materials were used as provided: Cab-O-Sil (Grade M5, Cabot) as the silica source, sodium aluminate ($NaAlO_2$, Wako) as the aluminum source, and sodium hydroxide solution (NaOH, 1 N solution or 50 w/v% in water, Wako) as the alkali source. For the synthesis of ferrierite and ZSM-11 seeds, pyridine (C_5H_5N, 99.5%, Wako) and tetrabutylammonium hydroxide (TBAOH, 40 wt % in water, Aldrich) were used as OSDAs, respectively.

Seed Crystals. In the present study, mordenite, ferrierite, ZSM-5, and ZSM-11 were used as seed crystals and were obtained by the following procedures. Mordenite: Na−mordenite (HSZ640NAA, SiO_2/Al_2O_3 = 18.0) supplied by Tosoh Corp. was used as provided. Ferrierite: Ferrierite was hydrothermally synthesized by reacting a mixture containing pyridine with the chemical composition $0.0875Na_2O$:0.6pyridine:$0.0167Al_2O_3$:SiO_2:$30H_2O$. The reactant mixture was prepared as follows: Sodium aluminate was dissolved in distilled water, followed by the addition of aqueous NaOH to obtain a clear solution. First pyridine and then Cab-O-Sil were added to the solution, and the mixture was stirred to obtain a homogeneous gel. The total weight of the gel was adjusted to 40 g. The mixture was transferred to a 60 mL stainless-steel autoclave and was then subjected to hydrothermal treatment at 165 °C for 72 h in an oven under autogenous pressure while being rotated at 20 rpm. After the hydrothermal treatment, the product was recovered by filtration, washed thoroughly with hot, distilled water, and dried at 60 °C. The residual pyridine in the zeolite was removed completely by calcination at 650 °C for 10 h in a stream of dry air. The product was identified by powder X-ray diffraction (XRD) as a crystalline ferrierite without impurities. The SiO_2/Al_2O_3 and Na_2O/Al_2O_3 ratios of the seeds determined by an inductively coupled plasma-atomic emission spectrometer (ICP-AES) were 32.0 and around unity, respectively. ZSM-5: Na−ZSM-5 (HSZ820NAA, SiO_2/Al_2O_3 = 23.8) supplied by Tosoh Corp. was used as provided. ZSM-11: The synthesis procedure was almost the same as that of ferrierite except for the use of tetrabutylammonium hydroxide (TBAOH) as an OSDA and the reactant mixture with the following chemical composition: $0.0125Na_2O$:$0.15TBA_2O$:$0.01Al_2O_3$:SiO_2:$14H_2O$. The hydrothermal treatment and calcination were performed at 180 °C for 96 h at 20 rpm and at 550 °C for 10 h, respectively. The product was identified by powder XRD as crystalline ZSM-11 without impurities. The SiO_2/Al_2O_3 and Na_2O/Al_2O_3 ratios of the seeds determined by the ICP analysis were 66.0 and 0.46, respectively.

Seed-Assisted, OSDA-Free Synthesis of Zeolites. All of the OSDA-free syntheses of zeolites in this study were carried out by adding the zeolite seeds to the starting Na−aluminosilicate gel with a chemical composition of $0.3Na_2O:0.01Al_2O_3:SiO_2:20H_2O$, which is the same as that of the typical gel used in our previous OSDA-free synthesis of zeolite beta (at point A in Figure 1). Here, the Na−aluminosilicate gel was prepared as follows: Sodium aluminate was dissolved in distilled water, followed by the addition of aqueous NaOH to obtain a clear solution. Next, a mixture of zeolite seeds and Cab-O-Sil was slowly added to the solution, which was kneaded using a mortar and pestle to obtain a homogeneous gel. Here, the added amount of zeolite seeds was 10 wt % relative to the silica source, and the total weight of the Na−aluminosilicate gel was adjusted to 18 g. Subsequently, the seeded Na−aluminosilicate gel was transferred to a 60 mL stainless-steel autoclave and subjected to hydrothermal treatment at 140−160 °C for different periods under autogenous pressure and static conditions. After the hydrothermal treatment, the product was recovered by filtration, washed thoroughly with hot, distilled water, and dried at 60 °C. The obtained solid products were characterized as their as-synthesized form. The solid yield of the obtained zeolite was defined as the weight ratio percentage (g/g × 100) of the dried solid product to the sum of the dry SiO_2, $NaAlO_2$, and the dry (calcined) seeds in the starting Na−aluminosilicate gel.

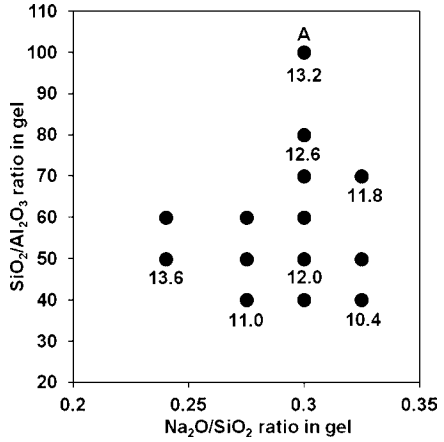

Figure 1. Crystallization area of beta obtained by the hydrothermal treatment of OSDA-free Na−aluminosilicate gel at 140 °C. The H_2O/SiO_2 ratio in the gels is 20−25. At the black point, beta is synthesized with good reproducibility. Inserted numerals indicate the SiO_2/Al_2O_3 ratios of the obtained beta products.

Characterization. Powder XRD patterns of the solid products were collected using a Mac Science MO3XHF22 diffractometer and Cu Kα radiation (λ = 0.15406 nm, 40 kV, 30 mA) from 5° to 40° in 2θ. The scanning step was 0.02° at a scanning speed of 2° min^{-1}. Elemental analyses of the zeolite seeds and products were performed by ICP-AES (Varian Liberty Series II) after dissolving them in hydrofluoric acid or potassium hydroxide solution. The crystal size and morphology were observed by a Hitachi S-4800 field-emission scanning electron microscope (FE-SEM). Nitrogen adsorption−desorption measurements of zeolite products were performed on Quantachrome Autosorb-1 at −196 °C. Prior to the measurements, all samples were degassed at 400 °C for 4 h under vacuum.

RESULTS AND DISCUSSION

Recapitulation of Previous Study. We have recently investigated the details of the seed-assisted, OSDA-free synthesis of beta in the Na−aluminosilicate gel system.[7,14] Highly crystalline beta with SiO_2/Al_2O_3 ratios of 10.4−13.6 were synthesized by hydrothermal treatment at 140 °C for 24−100 h from Na−aluminosilicate gels with a wide range of

dx.doi.org/10.1021/ja3022335 | J. Am. Chem. Soc. 2012, 134, 11542−11549

chemical compositions, as shown in Figure 1. The H_2O/SiO_2 ratio of the gels ranged from 20 to 25.[7] Beta crystallized only when beta seeds were added; alternatively, mordenite was obtained from the gel without seeds after a long hydrothermal treatment, typically from the gel at point A (Figure 1), as shown in Figure 2. The SiO_2/Al_2O_3 ratio and the solid yield of

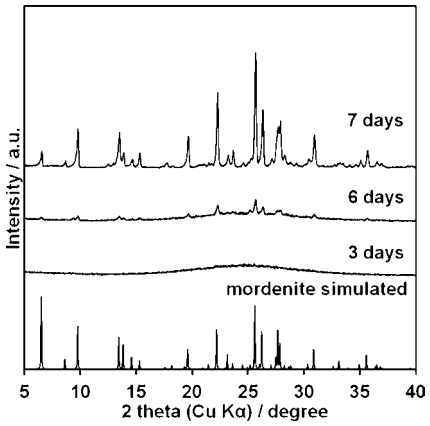

Figure 2. Evolution of the XRD patterns of the product from the seed-free gel at synthesis point A (in Figure 1) with hydrothermal treatment at 140 °C.

the mordenite obtained after 7 days were 13.6 and 18%, respectively. It was found that the beta seeds in the Na-aluminosilicate gel were partially dissolved during the hydrothermal treatment, and new beta crystals grew on the surface of the residual beta seeds by the supply of nutrients species via the liquid phase.[14] These nutrient species, coexisting with amorphous Na–aluminosilicate gel, are expected to play an important role in the crystallization of beta; however, it is difficult to identify these species by conventional techniques. Next, the effect of seeds with different zeolitic framework structures was examined with the Na–aluminosilicate gel having the same chemical composition as that used in the OSDA-free synthesis of beta (point A in Figure 1).

Seed-Assisted Syntheses Using Mordenite or Ferrierite Seeds. Figure 3 shows the XRD patterns of the products synthesized by the addition of mordenite seeds with different periods of hydrothermal treatment at 140 °C. Before heating (0 h), weak peaks attributed to mordenite seeds were observed, and only after 1 h of heating was evident crystal growth of mordenite observed. The maximum peak intensities of mordenite were attained after 12 h of heating, which is in contrast with the slow crystallization of mordenite from the seed-free gel with the same chemical composition (7 days, see Figure 2). Next, the ferrierite seeds were examined at 150 °C to understand the effect of the different framework structures of the zeolite seeds. Surprisingly, ferrierite also crystallized at a considerably rapid growth rate, as shown in Figure 4. After just

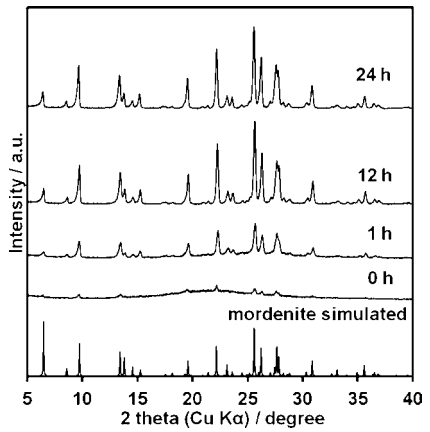

Figure 3. Evolution of the XRD patterns of the products from the gel with mordenite seeds at synthesis point A (in Figure 1) with hydrothermal treatment at 140 °C.

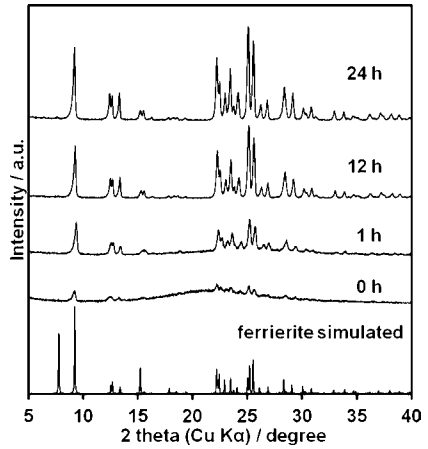

Figure 4. Evolution of the XRD patterns of the products from the gel with ferrierite seeds at synthesis point A (in Figure 1) with hydrothermal treatment at 150 °C.

1 h of heating, crystal growth was evident, and the ferrierite peaks reached maximum intensity after 24 h. The SEM images of the mordenite and ferrierite products are shown in Figure 5a

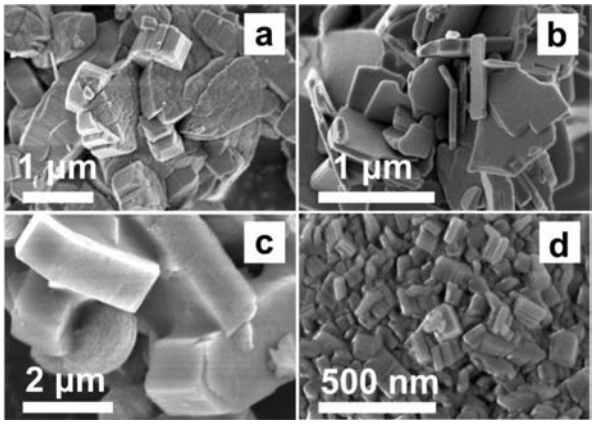

Figure 5. FE-SEM images of the aluminosilicate products: (a) mordenite, (b) ferrierite, (c) ZSM-5, and (d) ZSM-11, obtained by the seed-assisted, OSDA-free synthesis.

and b, respectively. The SiO_2/Al_2O_3 ratios of the obtained mordenite and ferrierite with maximum crystallinity were the same (15.2). The solid yields of these zeolites at maximum crystallinity were 20% and 22%, respectively, which are similar to that of beta (18%) obtained from the same starting gel. These results indicate that the nutrient species in the liquid phase coexisting with residual amorphous Na–aluminosilicate gel can contribute to the crystal growth of not only beta but also mordenite and ferrierite. Here, the nutrient species are

dx.doi.org/10.1021/ja3022335 | J. Am. Chem. Soc. 2012, 134, 11542–11549

apparently the numerous types of soluble aluminosilicate and/or silicate species with relatively smaller molecular weight. Because not all of the soluble species may facilitate the crystal growth of the specific zeolite, the nutrient species are recognized as precursors to zeolites. The crucial precursors are expected to depend on the type of zeolites, that is, the framework structures of the zeolites. On the basis of the above results, we considered that beta, mordenite, and ferrierite may have common key precursors for crystal growth, and that these three zeolites may have common structural parts in their frameworks, which provide us with clues regarding the crucial precursors to these three zeolites.

Common Composite Building Unit. In the reactant mixtures prior to the crystallization of zeolites, the existence of precursors containing specific ring structures has been reported in several studies.[20−24] Schueth et al. comprehensively investigated the precursors in the early stage of crystallization of all silica and germanosilicate zeolites from the starting gel containing OSDAs (TPA^+ for MFI, TEA^+ for BEC, and ROH for LTA, ROH = 4-methyl-2,3,6,7-tetrahydro-1*H*-5*H*-pyrido-[3.2.1-*ij*] quinolinium hydroxide, MFI, BEC, and LTA are the framework type code (FTC) of Silicalite-1, Beta polymorph C, and ITQ-29, respectively). The time dependence of the distribution of the precursors was monitored by electrospray ionization mass spectrometry.[20−22] Schueth et al. succeeded in the identification of the zeolite precursors with specific structures in the liquid phase of the gel prior to crystallization, which are the characteristic structural elements of the final zeolites. On the other hand, we have already proposed a schematic reaction model for the crystallization of zeolite A (LTA) and zeolite X (FAU), in which a four-membered ring (4R) for LTA and D6R for FAU were suggested to exist in the liquid phase of the gel prior to crystallization,[23,24] and these species were estimated to be identical to the above-mentioned critical zeolite precursors.

The three-dimensional framework structures of zeolites consist of secondary building units and/or composite building units, as summarized in the database of the Structure Commission of the International Zeolite Association (IZA-SC).[25] First, the ring distributions of beta, mordenite, and ferrierite were compared, and the common units turned out to be 5R and 12R, as shown in Figure 6, which can be also seen in many other zeolites. The result indicates that the common unit among the three zeolites should be considered at the level of higher units, that is, the composite building units. Currently, the number of approved composite building units is 47, and those contained in each framework structure type are also summarized in the database of the IZA-SC.[25] It is easily understood that beta (*BEA) contains the composite building units of *bea*, *mtw*, and *mor*, whereas mordenite (MOR) contains only the *mor* unit and ferrierite (FER) only the *fer* unit in their frameworks. It seems that there is no common composite building unit among these three zeolites; however, the *fer* unit consists of 13 T (T for tetrahedral = Si or Al) atoms and is decomposed into the *mor* unit and 5R, which consist of 8 and 5 T atoms, respectively, as illustrated in Figure 7. Consequently, the *mor* unit is elucidated as the common composite building unit of beta, mordenite, and ferrierite. It is reasonably understood the reason for the rapid crystallization of mordenite by the addition of mordenite seeds to the gel from which mordenite is crystallized in the absence of any seed, when it is assumed that the *mor* unit is the crucial precursor prior to crystallization of mordenite. Furthermore, by the same assumption, the crystallization behavior of beta and ferrierite by the addition of each seed to the gel from which mordenite is crystallized in the absence of any seed can be reasonably explained.

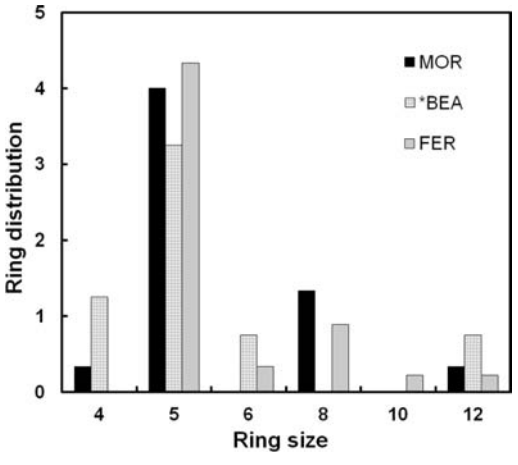

Figure 6. Ring distributions in MOR, *BEA, and FER.

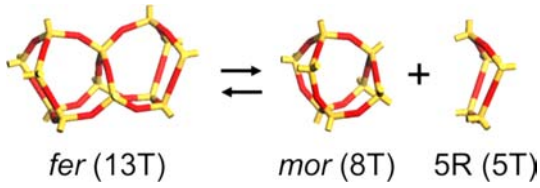

Figure 7. Structural correlation of the composite building units between *fer* and *mor*.

The crystal growth behavior of these three zeolites with the supply of the *mor* unit is estimated as follows. On the clean surface of the remaining seeds after partial dissolution of the external surface to expose the crystal surface, a *mor* unit in the liquid phase of the gel migrates to the specific site on the surface of the seed zeolite, and attaches to the terminal TOH, piling up as building blocks on the surface of the zeolite seed. After the multiple *mor* units are piled on the specific surface sites, other simple silicate and/or aluminosilicate molecules in the liquid phase of the gel fill up the space between the multiple *mor* units on the surface, and then a new zeolitic surface with the same framework structure as that of the seeds is generated. The migration and piling up of the *mor* units and filling of the space between the multiple *mor* units on the surface might proceed layer by layer, and zeolite crystal particles with clear crystal habits are expected to form subsequently. The obtained products in this study show their own clear crystal habit as shown in Figure 5. The crystal growth model applied to beta is illustrated in Supporting Information Figure 1.

The above speculative description helps us to imagine the crystallization behavior in the seed-assisted synthesis of zeolites. Because the composite building units are fictive molecular species taken from the framework of zeolites, they cannot be easily isolated as stable species. Furthermore, it is reported that the distribution of Al and Si atoms in the zeolitic framework is symmetrically ordered,[26−28] and the SiO_2/Al_2O_3 ratios of the obtained zeolites in this study are relatively low; therefore, the Al atoms in the *mor* unit and simple aluminosilicate molecules may play an important role in the crystal growth process.

dx.doi.org/10.1021/ja3022335 | *J. Am. Chem. Soc.* 2012, 134, 11542−11549

Clearly, the details of the entire mechanism are hard to deduce on the basis of the available data alone.

A Working Hypothesis. On the basis of the discussion on the common composite building units between the seed zeolite and the finally crystallized zeolite from the seed-free gel, the following working hypothesis is proposed to determine the synthesis condition. For the OSDA-free synthesis, a target zeolite should be added as seeds to a gel that yields a zeolite containing the common composite building unit when the gel is heated without seeds. According to this working hypothesis, the correlation of the common composite building unit between beta and mordenite is shown in Figure 8a. Beta

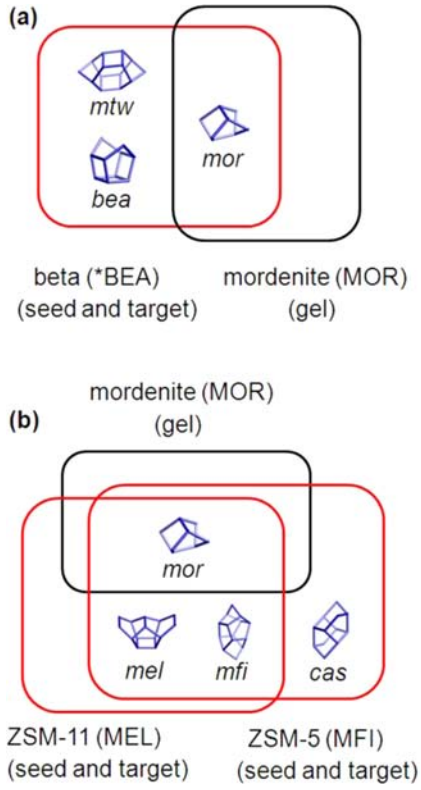

Figure 8. Correlation of common composite building unit between (a) MOR and *BEA, and (b) MOR, MFI, and MEL.

containing three composite building units, *mor*, *bea*, and *mtw*, can be synthesized with the addition of beta seeds into the OSDA-free reactant gel, which yield mordenite containing the common composite building unit *mor* when the gel without any seeds is heated. Furthermore, if the hypothesis is valid for the synthesis of other zeolites, ZSM-5 (MFI) and ZSM-11 (MEL) containing the *mor* building unit should be synthesized with the addition of these seeds into the same reactant gel that otherwise yields mordenite. The correlation of the composite building unit among ZSM-5, ZSM-11, and mordenite is shown in Figure 8b.

Syntheses of ZSM-5 and ZSM-11 by the Application of the Working Hypothesis. The seed-assisted, OSDA-free synthesis of ZSM-5 was performed at 160 °C, and the crystal growth of ZSM-5 was investigated by varying the time of the hydrothermal treatment. The maximum crystallinity of ZSM-5 with a trace amount of mordenite was observed after 20 h, and the growth of mordenite as an impurity phase was observed after 17 h (Figure 9). ZSM-11 was prepared at 140 °C, and the

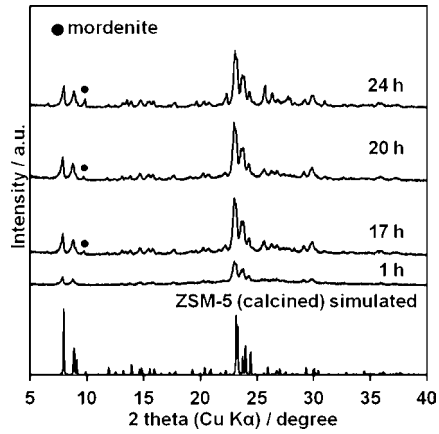

Figure 9. Evolution of the XRD patterns of the products from the gel with ZSM-5 seeds at point A (in Figure 1) with hydrothermal treatment at 160 °C. Filled symbols indicate the mordenite impurity.

maximum crystallinity of ZSM-11 with no impurities was observed after 15 h (Figure 10). These results indicate that,

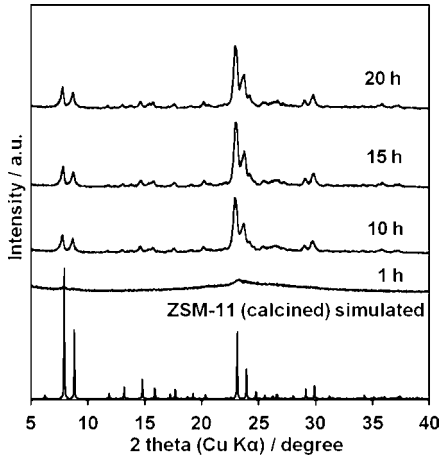

Figure 10. Evolution of the XRD patterns of the products from the gel with ZSM-11 seeds at point A (in Figure 1) with hydrothermal treatment at 140 °C.

similar to the case of beta, the crystal growth of ZSM-5 and ZSM-11 with the addition of the corresponding seeds is more rapidly accelerated than the spontaneous nucleation of mordenite. However, in the synthesis of ZSM-5 at 140 and 150 °C, the crystallization of mordenite started prior to the completion of ZSM-5 crystallization because of its slower crystal growth rate. The SiO_2/Al_2O_3 ratios of the obtained ZSM-5 and ZSM-11 with the maximum crystallinity were 18.6 and 17.6, respectively. The solid yields of ZSM-5 and ZSM-11 were 17% and 18%, respectively, which are almost the same as that of beta (18%).

The typical SEM image of the obtained ZSM-5 crystals (Figure 5c) shows a thick plate-like morphology with a size of several micrometers, and a small amount of amorphous material seems to remain in the interface of these crystals. Moreover, a spherical particle was seen in Figure 5c, which might be mordenite crystal as an impurity. This result was also evidenced by the XRD pattern in Figure 9. On the other hand, a typical SEM image of ZSM-11 crystals shows aggregates of 50−150 nm crystals with tetragonal morphology, as depicted in Figure 5d. The BET surface area, micropore surface area, and

dx.doi.org/10.1021/ja3022335 | J. Am. Chem. Soc. 2012, 134, 11542−11549

the micropore volume of these two zeolites with the highest crystallinity were calculated by the *t*-plot method from nitrogen adsorption data, and the chemical compositions of the products and seeds are listed in Table 1. The micropore surface area and pore volume of the obtained ZSM-5 are slightly smaller than those of the seeds, and the values for ZSM-11 are almost the same as those for the seeds. These results show that crystalline Al-rich ZSM-5 and ZSM-11 can be obtained using the procedure of the proposed working hypothesis. To the best of our knowledge, this is the first report on the synthesis of ZSM-11 under completely OSDA-free conditions. Moreover, it is the first on the OSDA-free synthesis of ZSM-5 with a SiO_2/Al_2O_3 ratio below 22.

Table 1. SiO_2/Al_2O_3 Ratios and Pore Characteristics of ZSM-5 and ZSM-11 Products and Their Seeds

sample	SiO_2/Al_2O_3[a]	BET surface area [$m^2\ g^{-1}$]	micropore surface area [$m^2\ g^{-1}$][b]	micropore volume [$cm^3\ g^{-1}$][b]
ZSM-5 product (20 h)	18.6	307	180	0.10
ZSM-11 product (15 h)	17.6	326	220	0.12
ZSM-5 seeds	23.8	316	212	0.11
ZSM-11 seeds	66.0	426	196	0.12

[a]Determined by ICP-AES. [b]Determined by the *t*-plot method.

The SiO_2/Al_2O_3 ratios of the seeds and zeolite products, and the solid yield of the products as well as those values of mordenite from the gel without any seeds heated at 140 °C for 7 days (shown in Figure 2) are summarized in Table 2. The effect of the SiO_2/Al_2O_3 ratio of the seeds in the synthesis of each zeolite was not fully investigated except for the beta synthesis;[7] however, the suitable SiO_2/Al_2O_3 ratio of the seed zeolites seems to be different for each zeolite type, as shown in Table 2. The reason for this variation is thought to be the difference in the solubility of the seed zeolite in the caustic gel during hydrothermal treatment, which is mainly attributed to the amount of defects in the zeolitic framework, the distribution of Al and Si atoms in the zeolitic framework, and the particle size of the seed crystals. The SiO_2/Al_2O_3 ratios and solid yields of the product zeolites converged in the relatively narrow range of 13.2−18.6 and 17−22%, respectively, as shown in Table 2. In this study, as the proportion of the seeds in the solid reactant mixture (dry SiO_2, $NaAlO_2$, and dry (calcined) seeds) is 8.7%, around one-half or more than one-half the amount of the product zeolite crystals is newly synthesized from the reactant gel in all cases. All of the zeolite products from the seeded gels show lower SiO_2/Al_2O_3 ratios (13.2−18.6) than those of their seeds. The result indicates that the newly synthesized zeolite crystals with SiO_2/Al_2O_3 ratio similar to that of mordenite from seed-free gel (13.6) grow on the surface of the seeds. The low solid yield of zeolites from seeded gels (17−22%) similar to that value of mordenite from seed-free gel (18%) is attributed to the dissolution of much amount of silica in the synthesis gel into liquid phase because of the higher ratios of SiO_2/Al_2O_3 (=100) and Na_2O/SiO_2 (=0.3) of the synthesis gel as described in the Experimental Section as compared to those values in the typical synthesis of Al-rich zeolites. Consequently, the SiO_2/Al_2O_3 ratio and the solid yield of obtained zeolites are determined by the chemical composition of the synthesis gel.

Table 2. SiO_2/Al_2O_3 Ratios of Seeds and Product Zeolites, and Solid Yield in Seed-Assisted, OSDA-Free Synthesis of Zeolites

zeolites	SiO_2/Al_2O_3 (seeds)[a]	SiO_2/Al_2O_3 (product)[a]	solid yield of product [%][b]
beta	24.0	13.2	18
mordenite	18.0	15.2	20
ferrierite	32.0	15.2	22
ZSM-5	23.8	18.6	17
ZSM-11	66.0	17.6	18
mordenite[c]		13.6	18

[a]Determined by ICP-AES. [b]The solid yield (g/g × 100%) of the product was calculated from the weight ratio of dried solid product to the sum of dry weight of SiO_2, $NaAlO_2$, and dry (calcined) seeds in the starting sodium aluminosilicate gel. [c]Obtained from the gel without seeds at 140 °C for 7 days.

Application of the Working Hypothesis to the Syntheses of Other Zeolites. Considering the framework structure and the composite building units of zeolites, the correlation of those in the seed-assisted synthesis of ZSM-12 (MTW) from the gel, yielding ZSM-5 when the gel is heated without seeds for a long time, is shown in Figure 11a. The results have been already reported in another study,[11] in which Na-ZSM-12-type zeolites with SiO_2/Al_2O_3 ratios from 23.4 to 32.4 were successfully obtained. This is the first application of

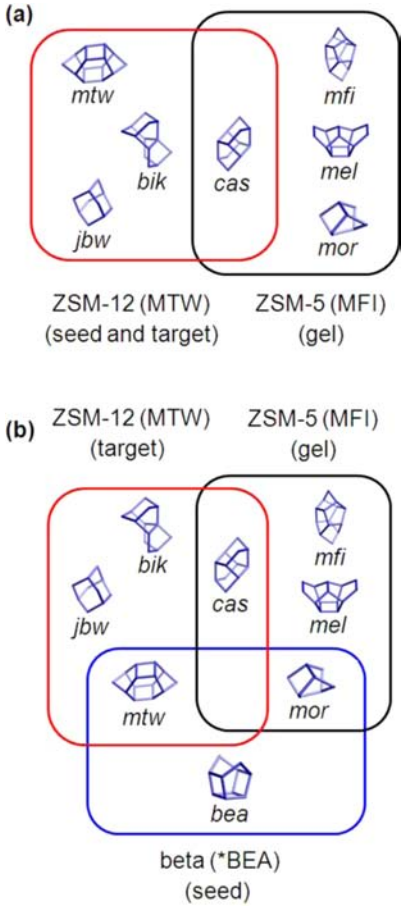

Figure 11. Correlation of common composite building units between (a) MFI and MTW, and (b) MFI, *BEA, and MTW.

dx.doi.org/10.1021/ja3022335 | J. Am. Chem. Soc. 2012, 134, 11542−11549

our hypothesis that involves *cas*, instead of *mor*, as the common composite building unit. From the gel without ZSM-12 seeds, ZSM-5 and mordenite were obtained after prolonged heating; however, only ZSM-5 was obtained in the early stages of crystallization.[11] It is speculated that the fictive *cas* unit, as the common composite building unit, effectively contributes to the crystal growth of ZSM-12.

Another example is the case in which the framework types of target and seed zeolites are not the same; that is, the target zeolite is ZSM-12, the seed zeolite is beta, and the gel is for ZSM-5, as illustrated in Figure 11b. The hypothesis was based on the structural similarity between MTW, BEA, and BEB (here, BEB is not officially used for the FTC in the database of the IZA-SC,[25] and BEB is just used for the convenience of understanding the similarity in the framework structure between ZSM-12 and beta). The *a*−*c* projections of the frameworks of MTW, BEA, and BEB perpendicular to the straight 12MR are very similar to each other as reported in previous studies.[29,30] Na-ZSM-12 was successfully synthesized by combining the *mtw* building unit from the beta seeds as the growth surface and the *cas* building unit as the nutrient species from the seed-free gel for the synthesis of ZSM-5. The results are reported in a separate paper.[31]

One more new application of the hypothesis is the synthesis of ECR-18 (PAU) in the K−aluminosilicate system in which the calcined seeds of ECR-18 were added to the gel that yields Linde W (MER) without seeds. The correlation of the common composite units between MER and PAU is illustrated in Supporting Information Figure 2. The experimental results of the syntheses Linde W as the final product from the seed-free gel, ECR-18 seeds, and ECR-18 by OSDA-free synthesis are presented in Supporting Information Figures 3 and 4. Although Linde W obtained from the seed-free gel is contaminated by a small amount of zeolite L as shown in Supporting Information Figure 3, the ECR-18 by OSDA-free synthesis is pure phase, and not containing zeolite L as shown in Supporting Information Figure 4. ECR-18 crystallizes in pure phase from the gel with higher SiO_2/Al_2O_3 ratio than that with lower SiO_2/Al_2O_3 ratio from which pure Linde W crystallizes without seeds. When the seeds of ECR-18 were added to the gel from which pure Linde W was crystallized without seeds, the obtained ECR-18 contained a small amount of Linde W. This result is the typical example of the optimization of the gel composition in the seed-assisted synthesis of zeolite without OSDA, and the correlation of common composite building units between the target zeolite and other zeolite obtained from the seed-free gel is fundamentally maintained. Detailed characterizations as well as the synthesis conditions for ECR-18 obtained from seed-assisted synthesis without OSDA will be reported in a separate paper in the near future.

Finally, the requirements for a successful seed-assisted, OSDA-free synthesis of zeolites to broaden the zeolite types on the basis of the proposed hypothesis are summarized as follows: (1) the spontaneous nucleation should not occur prior to the completion of the crystal growth of the target zeolite; (2) the precursor, the common composite building unit, must access the top surface of the seed zeolite; (3) the zeolite seeds should not completely dissolve prior to the onset of crystal growth during the hydrothermal treatment, and the SiO_2/Al_2O_3 ratio of the seeds should be optimized; (4) when the framework structure of the target and the seed zeolites is the same, the seeds should have at least one common composite building unit with the zeolite to be synthesized from the gel without seeds; and (5) the chemical composition of the gel to which the seeds are added should be optimized.

The validity of the working hypothesis is supported by the successful syntheses of some aluminosilicate zeolites, as described above. Furthermore, the application of the proposed methodology to zeolite synthesis, including nonaluminosilicate zeolites, is under investigation and will be reported elsewhere.

CONCLUSION

We proposed a working hypothesis for the seed-assisted, OSDA-free synthesis of zeolites on the basis of the results of OSDA-free synthesis of beta, mordenite, and ferrierite, and the structural consideration of the common composite building units between the seed zeolite and the zeolites obtained from seed-free gels. By applying the hypothesis, the seed-assisted, OSDA-free synthesis was successfully achieved on ZSM-5, ZSM-11, and ZSM-12. Furthermore, the other successful route to the OSDA-free synthesis of ZSM-12 with the aid of beta seeds was reasonably explained by considering the combination of composite building units (*mtw* + *cas*) in the beta seeds (*mtw*) and the gel-yielding ZSM-5 (*cas*) when no seeds were added. The requirements for a successful seed-assisted, OSDA-free synthesis of zeolites are proposed on the basis of the synthesis results. Although the validity of the proposed hypothesis is supported by some Na−aluminosilicate zeolites and K−aluminosilicate ECR-18 described here, further broadening of zeolite types by seed-assisted, OSDA-free synthesis will be realized by applying the proposed working hypothesis in the near future, and already some success has been achieved in this regard.

ASSOCIATED CONTENT

Supporting Information

Schematic crystal growth model applied to the seed-assisted, OSDA-free synthesis of zeolite beta, common composite building unit between ECR-18 and Linde W, the seed-assisted synthesis of ECR-18, and the results. This material is available free of charge via the Internet at http://pubs.acs.org.

AUTHOR INFORMATION

Corresponding Author

okubo@chemsys.t.u-tokyo.ac.jp

Notes

The authors declare no competing financial interest.

ACKNOWLEDGMENTS

We acknowledge Nippon Chemical Industrial Co. Ltd. for chemical analyses, nitrogen adsorption−desorption measurements, and FE-SEM. This study was financially supported in part by Nippon Chemical Industrial Co. Ltd., a Grant-in-Aid for Scientific Research (B) from the Japan Society for the Promotion of Science (JSPS), and a Grant-in-Aid for Young Scientists from the JSPS. Y.K. gratefully thanks the JSPS for a postdoctorial fellowship and a Grant-in-Aid for Scientific Research. K.I. gratefully thanks the JSPS for a Grant-in-Aid for Scientific Research.

REFERENCES

(1) Breck, D. W. *Zeolite Molecular Sieves*; Wiley: New York, 1974.
(2) Davis, M. E.; Lobo, R. F. *Chem. Mater.* **1992**, *4*, 756−768.
(3) Corma, A. *Chem. Rev.* **1997**, *97*, 2373−2419.

(4) Auerbach, S. M., Carrado, K. A., Dutta, P. K., Eds. *Handbook of Zeolite Science and Technology*; Marcel Dekker: New York, 2003.
(5) Xie, B.; Song, J.; Ren, L.; Ji, Y.; Li, J.; Xiao, F.-S. *Chem. Mater.* **2008**, *20*, 4533−4535.
(6) Majano, G.; Delmotte, L.; Valtchev, V.; Mintova, S. *Chem. Mater.* **2009**, *21*, 4184−4191.
(7) Kamimura, Y.; Chaikittisilp, W.; Itabashi, K.; Shimojima, A.; Okubo, T. *Chem. Asian J.* **2010**, *5*, 2182−2191.
(8) Majano, G.; Darwiche, A.; Mintova, S.; Valtchev, V. *Ind. Eng. Chem. Res.* **2009**, *48*, 7084−7091.
(9) Yokoi, T.; Yoshioka, M.; Imai, H.; Tatsumi, T. *Angew. Chem., Int. Ed.* **2009**, *48*, 9884−9887.
(10) Iyoki, K.; Kamimura, Y.; Itabashi, K.; Shimojima, A.; Okubo, T. *Chem. Lett.* **2010**, *39*, 730−731.
(11) Kamimura, Y.; Itabashi, K.; Okubo, T. *Microporous Mesoporous Mater.* **2012**, *147*, 149−156.
(12) Zhang, H.; Guo, Q.; Ren, L.; Yang, C.; Zhu, L.; Meng, X.; Li, C.; Xiao, F -S. *J. Mater. Chem.* **2011**, *21*, 9494−9497.
(13) Xie, B.; Zhang, H.; Yang, C.; Liu, S.; Ren, L.; Zhang, L.; Meng, X.; Yilmaz, B.; Müller, U.; Xiao, F.-S. *Chem. Commun.* **2011**, *47*, 3945−3947.
(14) Kamimura, Y.; Tanahashi, S.; Itabashi, K.; Shimojima, A.; Okubo, T. *J. Phys. Chem. C* **2011**, *115*, 744−750.
(15) Kerr, G. T. *J. Phys. Chem.* **1968**, *72*, 1385−1386.
(16) Kasahara, S.; Itabashi, K.; Igawa, K. *Stud. Surf. Sci. Catal.* **1986**, *28*, 185−192.
(17) Edelman, R. D.; Kudalkar, D. V.; Ong, T.; Warzywoda, J.; Thompson, R. W. *Zeolites* **1989**, *9*, 496−502.
(18) Dutta, P. K.; Bronic, J. *Zeolites* **1994**, *14*, 250−255.
(19) Gora, L.; Streletzky, K.; Thompson, R. W.; Phillies, G. D. G. *Zeolites* **1997**, *19*, 98−106.
(20) Pelster, S. A.; Schrader, W.; Schueth, F. *J. Am. Chem. Soc.* **2006**, *128*, 4310−4317.
(21) Pelster, S. A.; Kalamajka, R.; Schrader, W.; Schueth, F. *Angew. Chem., Int. Ed.* **2007**, *46*, 2299−2302.
(22) Schaack, B. B.; Schrader, W.; Schueth, F. *Angew. Chem., Int. Ed.* **2008**, *47*, 9092−9095.
(23) Ogura, M.; Kawazu, Y.; Takahashi, H.; Okubo, T. *Chem. Mater.* **2003**, *15*, 2661−2667.
(24) Iwama, M.; Suzuki, Y.; Plevert, J.; Itabashi, K.; Ogura, M.; Okubo, T. *Cryst. Growth Des.* **2010**, *10*, 3471−3479.
(25) http://www.iza-structure.org/databases.
(26) Takaishi, T.; Kato, M.; Itabashi, K. *Zeolites* **1995**, *15*, 21−32.
(27) Takaishi, T. *J. Phys. Chem.* **1995**, *99*, 10982−10987.
(28) Kato, M.; Satokawa, S.; Itabashi, K. *Stud. Surf. Sci. Catal.* **1997**, *105*, 229−235.
(29) Lobo, R. F.; Tsapatsis, M.; Freyhardt, C. C.; Chan, I.; Chen, C.-Y.; Zones, S. I.; Davis, M. E. *J. Am. Chem. Soc.* **1997**, *119*, 3732−3744.
(30) Kubota, Y.; Honda, T.; Plevert, J.; Yamashita, T.; Okubo, T.; Sugi, Y. *Catal. Today* **2002**, *74*, 271−279.
(31) Kamimura, Y.; Iyoki, K.; Elangovan, S. P.; Itabashi, K.; Shimojima, A.; Okubo, T. *Microporous Mesoporous Mater.*, in press.